Journal of Earthquake and Tsunami
Vol. 6, No. 4 (2012) 1250025 (21 pages)

DOI: 10.1142/S179343111250025X

SEISMIC RESPONSE OF POWER TRANSMISSION TOWER-LINE SYSTEM UNDER MULTI-COMPONENT MULTI-SUPPORT EXCITATIONS

TIAN LI*,†, LI HONGNAN† and LIU GUOHUAN‡

*School of Civil and Hydraulic Engineering
Shandong University, Jinan 250061, China

†State Key Laboratory of Coastal and Offshore Engineering
Dalian University of Technology, Dalian 116024, China

‡Department of Civil Engineering
Tsinghua University, Beijing 100084, China

Received 13 May 2011
Accepted 14 September 2011
Published 4 September 2012

The effect of multi-component multi-support excitations on the response of power transmission tower-line system is analyzed in this paper, using three-dimensional finite element time-stepping analysis of a transmission tower-line system based on an actual project. Multi-component multi-support earthquake input waves are generated based on the Code for Design of Seismic of Electrical Installations. Geometric non-linearity was considered in the analysis. An extensive parametric study was conducted to investigate the behavior of the transmission tower-line system under multi-component multi-support seismic excitations. The parameters include single-component multi-support ground motions, multi-component multi-support ground motions, the correlations among the three-component of multi-component multi-support ground motions, the spatial correlation of multi-component multi-support ground motions, the incident angle of multi-component multi-support seismic waves, the ratio of the peak values of the three-component of multi-component multi-support ground motions, and site condition with apparent wave velocity of multi-component multi-support ground motions.

Keywords: Power transmission tower-line system; geometric nonlinearity; multi-component multi-support ground motions; apparent wave velocity.

1. Introduction

Power transmission tower-line system is an important facility of a power system. Its failure may lead to the outage of power supply. Until now, much of research effort has been focused on the actions of static load, impulsive load, and equivalent static wind load [American Society of Civil Engineerings Committee on Electrical Transmission Structures, 1982; American Society of Civil Engineerings, 1991; Mozer *et al.*, 1977]. Only very few studies have dealt with the dynamic load. Design codes such as the code for Design of Seismic of Electrical Installations (GB 50260-96) [Ministry of China Electrical Industry, 1996] and the Design Regulations on 110 ∼ 500 kv Overhead Transmission Line (DL/T 5092-1999) [Huadong Electrical Power

Design Institute, 1999] do not provide guidelines on how to consider the effects of lines in seismic analysis of transmission tower-line system.

There have been several cases of damage to transmission towers and lines during earthquakes. For instance, during the 1992 Landers earthquake, about 100 lines were broken [Hall *et al.*, 1995] in the city of Los Angeles. During the 1995 Kobe earthquake, 38 transmission lines were damaged and 20 towers tilted as a result of foundation settlement [Shinozuka, 1995]. In the 1999 Chi–Chi earthquake, many lines were broken and some towers collapsed [Yin *et al.*, 2005]. Figure 1 shows some pictures of damaged towers in Sichuan electric network during the 2008 Wenchuan earthquake in China.

In the past one or two decades, some research has been conducted to develop simplified analytical approaches for transmission tower-line system. For instance, Li *et al.* [Li *et al.*, 2003, 2004, 2005] have completed a number of studies on seismic effects on transmission towers and have verified that the effect of lines in seismic design should not be neglected. Ghobarah *et al.* [1996] investigated the effects of multi-support excitations on the response of overhead power transmission lines. They modeled the transmission towers using space truss elements and the cables by straight two node elements, in which the system was subjected to spatially incoherent seismic ground motions. Tian *et al.* [2008] synthesized multi-support time histories of earthquake ground motion and analyzed the power transmission tower-line system under multi-support excitations considering traveling-wave and coherency effect, and the results showed that it was necessary to consider multiple support excitations in transmission tower-line system analysis. In all these studies, the transmission tower-line systems were assumed to be subjected to single-component excitation.

Longitudinally extended structures such as lifeline systems are often multi-supported and each support is subjected to multi-component ground motions during an earthquake. To date, seismic behavior of the transmission tower-line system subjected to multi-component excitations has not been investigated. This paper deals with such an analysis using three-dimensional finite element model. The multi-component multi-support earthquake input waves are generated based on the Code for Design of Seismic of Electrical Installations [Ministry of China

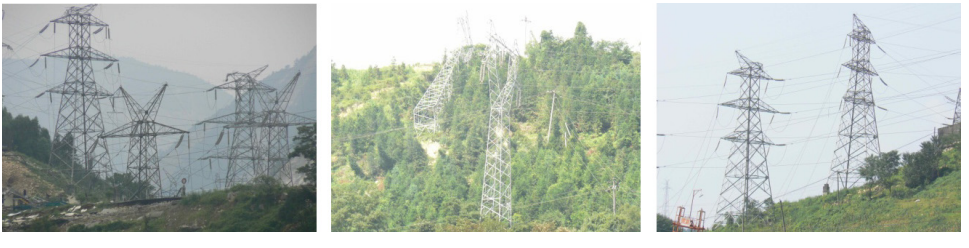

Fig. 1. Pictures of Wenchuan earthquake damage to transmission tower-line system.

Electrical Industry, 1996]. The time domain analysis takes into account geometric non-linearity due to finite deformation. The parameters studied include single-component multi-support ground motions, multi-component multi-support ground motions, the correlations among the three-component of multi-component multi-support ground motions, the spatial correlation of multi-component multi-support ground motions, the incident angle of multi-component multi-support seismic waves, the ratio of the peak values of the three-component of multi-component multi-support ground motions, and site condition with apparent wave velocity of multi-component multi-support ground motions.

2. Power Transmission Tower-Line System Model

2.1. *Structural model*

The three-dimensional finite element model is created based on an actual transmission tower-line system in Gaizhou City of Liaoning Province, China. The analysis was conducted using the SAP2000 finite element program. As shown in Fig. 2, the power transmission tower-line system consisted of 3 towers, 8 ground lines, and 24 conductor lines (three towers and four-span lines). The three towers and four-span lines model has been demonstrated that can obtain relative accurate responses [Tian *et al.*, 2010]. Each of the 53.9-m-high towers was constructed from steel angle sections with the elastic modulus of 206 Gpa, and weighs approximately 19.95 tonnes. Each tower was modeled by 6600 space beam members and 272 nodes. Connections between members were assumed to be rigid. Conductor line and ground line properties are listed in Table 1. The transmission line was modeled by 400 two-noded iso-parametric cable elements with three translational degrees-of-freedom at each node. The upper 8 cables are ground lines and lower 24 cables are four-bundled conductor lines. The distance between adjacent towers is 400 m. The base nodes of the transmission tower were fixed on the ground and the connections between transmission towers and lines were hinged. The space beam element was not divided

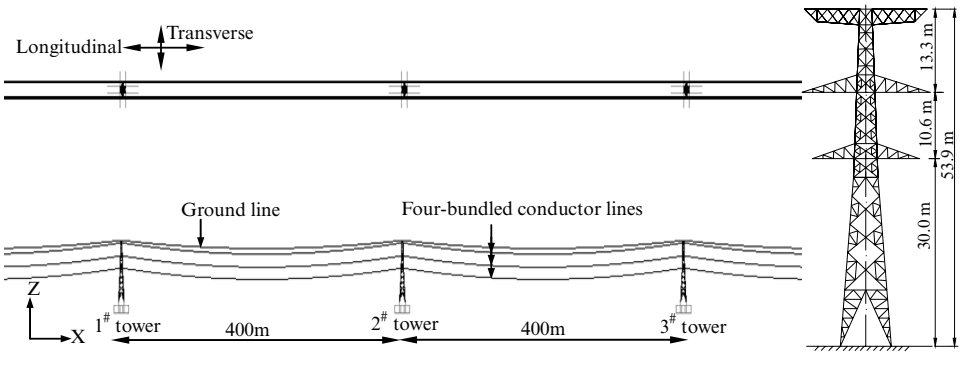

Fig. 2. Three-dimensional model of three towers and four-span lines coupled system.

Table 1. Conductor line and ground line properties.

Type	Conductor line	Ground line
Transmission line	LGJ-400/35 Aluminium conductor steel reinforced	LGJ-95/55 Aluminium conductor steel reinforced
Outside diameter (m)	26.82E-3	16.00E-3
Modulus (Gpa)	65	105
Transversal cross-section (m^2)	425.24E-6	152.81E-6
Mass per unit length (Kg/m)	1.3490	0.6967
Line expansion coefficient (1/°C)	2.05E-005	1.55E-005

and every transmission line was divided into 400 elements. The side spans of the lines are hinged at the same height of middle tower.

Under self-weight, the cables' configuration is a catenary. Based on the coordinate system illustrated in Fig. 3, Eq. (1) was used to define the initial geometry of the cable profile [Shen *et al.*, 1997],

$$z = \frac{H}{q}\left|\cosh(\alpha) - \cosh\left|\frac{2\beta x}{l} - \alpha\right|\right|, \tag{1}$$

where $\alpha = \sinh^{-1}|\frac{\beta(c/l)}{\sin(\beta)}| + \beta$, $\beta = \frac{ql}{2H}$, H represents the initial horizontal tension which can be obtained from a preliminary static analysis, and q denotes the uniformly distributed gravity loads along the transmission line.

2.2. *Geometric stiffness matrix of cable element*

As shown in Fig. 4, by resolution of force, the lateral forces $\{F_i\, F_j\}$ on a cable element of length L can be readily related to its lateral displacements $\{v_i\, v_j\}$ and the cable tension T via the relation [Wilson, 2002],

$$\begin{bmatrix} F_i \\ F_j \end{bmatrix} = \frac{T}{L}\begin{bmatrix} 1 & -1 \\ -1 & 1 \end{bmatrix}\begin{bmatrix} v_i \\ v_j \end{bmatrix} = k_g \begin{bmatrix} v_i \\ v_j \end{bmatrix}. \tag{2}$$

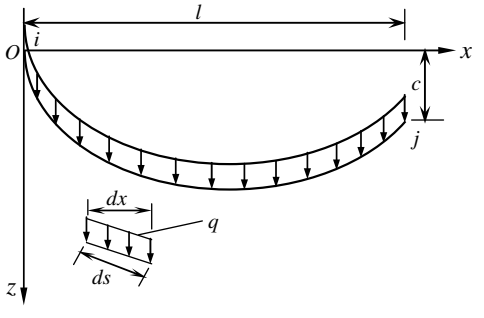

Fig. 3. Coordinates of a single cable under self-weight.

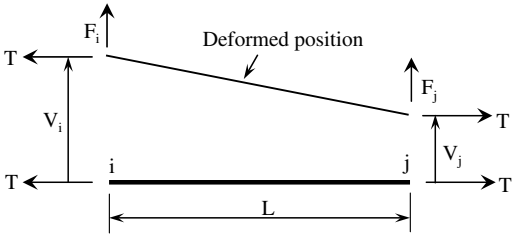

Fig. 4. Force acting on a cable element.

Note that k_g is only a function of the element's length and the force in the element. The cables have significant geometric non-linearity because large displacement of the cable changes its stiffness and its frequencies of free vibration [Ghobarah *et al.*, 1996]. Therefore, transmission lines should be treated as non-linear structures.

2.3. *Structural dynamic characteristic*

Figures 5(a) and 5(b) show the primary modal frequencies of a tower without transmission lines, and Figs. 5(c) and 5(d) show the modes of towers coupled with transmission lines, which are equivalent to the primary modal frequencies of a tower without transmission lines. Table 1 shows the primary modal frequencies of a tower without and with transmission lines. The primary modal frequencies of a single tower in the transverse and longitudinal directions are approximately 1.9 Hz. As shown in Table 2, the modal frequencies of towers coupled with transmission lines are lower than the corresponding frequencies without transmission lines. Hence, the effect of transmission lines on the vibrations of transmission tower should be not neglected. The results are similar to previous researches [Yasui *et al.*, 1999].

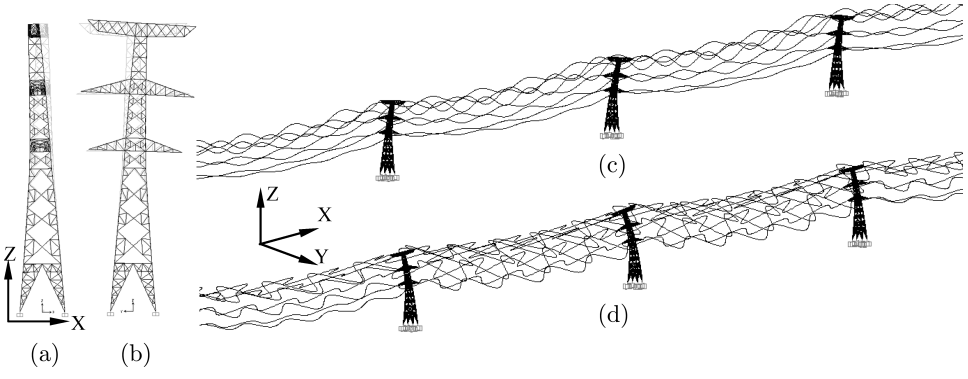

Fig. 5. Vibration modes of a tower without transmission lines and towers coupled with transmission lines. (a) Longitudinal direction (b) Transverse direction (c) Longitudinal direction (d) Transverse direction.

Table 2. The primary modal frequencies of a tower without and with transmission lines.

Vibration mode	Direction	The modal frequencies of a single tower without transmission lines (Hz)	The modal frequencies of towers coupled with transmission lines (Hz)	Relative error
First	Longitudinal	1.8951	1.6527	12.8%
	Transverse	1.8621	1.7191	7.68%

3. Simulation of Multi-Component Multi-Support Ground Motions

3.1. *Effect of the correlations among the three-component of multi-component ground motions*

According to research by Penzien and Watable [1975], the three components of ground motion along a set of principal axes are uncorrelated. These components, directed along the principal axes, are usually such that the major principal axis is directed towards the expected epicenter, the moderate principal axis is directed perpendicular to it and the minor principal axis is directed vertically.

As shown in Fig. 6, suppose that the angle between the direction of the major principal axis and the direction of wave propagation is α in this study. The direction of wave propagation is assumed to coincide with the longitudinal direction of transmission tower-line system. $\{\ddot{U}(\omega)\}$ is the acceleration vector in the xyz coordinate system, and $\{\ddot{U}_g(\omega)\}$ is the acceleration vector of the principal axes of ground motion, that is

$$\{\ddot{U}(\omega)\} = [\ddot{u}_x(\omega), \ddot{v}_y(\omega), \ddot{w}_z(\omega)]^T \tag{3}$$

$$\{\ddot{U}_{\mathrm{g}}(\omega)\} = [\ddot{u}_{\mathrm{g}}(\omega), \ddot{v}_{\mathrm{g}}(\omega), \ddot{w}_{\mathrm{g}}(\omega)]^T \tag{4}$$

Equations (3) and (4) can be expressed as [Li, 2006],

$$\{\ddot{U}(\omega)\} = [A]\{\ddot{U}_g(\omega)\}, \tag{5}$$

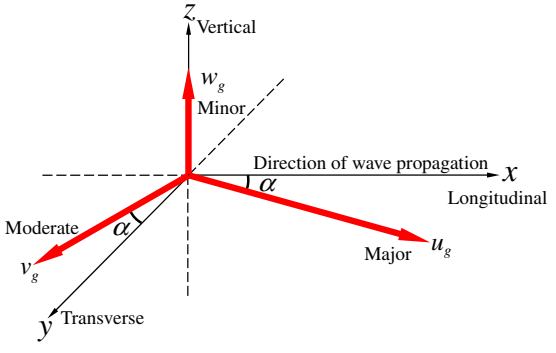

Fig. 6. Layout of the principal axes of ground motion and the direction of wave propagation.

where

$$[A] = \begin{bmatrix} \cos\alpha & -\sin\alpha & 0 \\ \sin\alpha & \cos\alpha & 0 \\ 0 & 0 & 1 \end{bmatrix}. \tag{6}$$

The cross-spectral matrix in the *xyz* coordinate system can be obtained as follows

$$\{S_{\ddot{U}}(\omega)\} = E[\{\ddot{U}(\omega)\}\{\ddot{U}(\omega)\}^T] = [A]\{S_{\ddot{U}_g}(\omega)\}[A]^T, \tag{7}$$

where $\{S_{\ddot{U}_g}(\omega)\}$ is the power spectral matrix of the principal axes.

The power spectral density (PSD) function of ground acceleration is defined by Clough and Penzien [1975] as:

$$S_{\ddot{f}_g\ddot{f}_g}(\omega) = \frac{\omega_g^4 + 4\varsigma_g^2\omega_g^2\omega^2}{(\omega_g^2 - \omega^2)^2 + 4\varsigma_g^2\omega_g^2\omega^2} \cdot \frac{\omega^4}{(\omega_f^2 - \omega^2)^2 + 4\varsigma_f^2\omega_f^2\omega^2} \cdot S_0 \tag{8}$$

in which ω_f and ς_f are the central frequency and damping ratio of the high pass filter, respectively. ω_g and ς_g are the central frequency and damping ratio of the Tajimi–Kanai PSD function, respectively. S_0 is a scale factor depending on the ground motion intensity.

Acceleration power spectrums of the principal axes are defined as:

$$S_{\ddot{u}_g}(\omega) = R_u^2 S_{\ddot{f}_g\ddot{f}_g}(\omega); \quad S_{\ddot{v}_g}(\omega) = R_v^2 S_{\ddot{f}_g\ddot{f}_g}(\omega); \quad S_{\ddot{w}_g}(\omega) = R_w^2 S_{\ddot{f}_g\ddot{f}_g}(\omega) \tag{9}$$

and its variances can be given by:

$$\sigma_{\ddot{u}_g}^2 = R_u^2\sigma_{\ddot{f}_g}^2; \quad \sigma_{\ddot{v}_g}^2 = R_v^2\sigma_{\ddot{f}_g}^2 \quad \sigma_{\ddot{w}_g}^2 = R_w^2\sigma_{\ddot{f}_g}^2, \tag{10}$$

where R_u, R_v, and R_w are the ratio factors.

The correlation between the various components of ground motion can be expressed as:

$$\rho_{ij}^2(\omega) = \frac{|S_{ij}(\omega)|^2}{S_{ii}(\omega)S_{jj}(\omega)} (0 \le \rho_{ij}^2(\omega) \le 1). \tag{11}$$

The coherency function matrix between the various components is given by:

$$[\rho(\omega)] = \begin{bmatrix} 1 & \rho_{12}(\omega) & \rho_{13}(\omega) \\ \rho_{21}(\omega) & 1 & \rho_{23}(\omega) \\ \rho_{31}(\omega) & \rho_{32}(\omega) & 1 \end{bmatrix} \tag{12}$$

The correlation coefficient between the two horizontal components of ground motion for the above model can be derived as:

$$\rho_{12}(\omega) = \rho_{21}(\omega) = \frac{|S_{\ddot{u}_x\ddot{u}_y}(\omega)|}{\sqrt{S_{\ddot{u}_x\ddot{u}_x}(\omega)S_{\ddot{u}_y\ddot{u}_y}(\omega)}} = \frac{|(1-a)\sin 2\alpha|}{\sqrt{(1+a)^2 - (1-a)^2\cos^2 2\alpha}}, \tag{13}$$

where $a = S_{\ddot{u}_g}(\omega)/S_{\ddot{v}_g}(\omega) = R_u^2/R_v^2$.

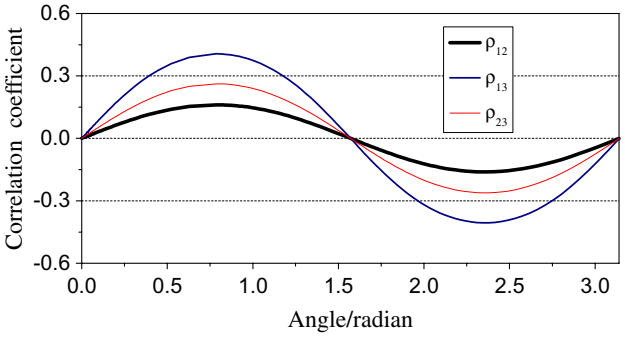

Fig. 7. Correlation between the various components.

Table 3. Correlation coefficients under different angles.

Angle	ρ_{12}	ρ_{13}	ρ_{23}
0°	0	0	0
18°	0.095	0.253	0.158
45°	0.161	0.406	0.262

The expression is plotted in Fig. 7 for selected values of $R_u : R_v : R_w = 1 : 0.85 : 0.65$. Table 3 shows the correlation coefficients under different angles.

3.2. *Coherency loss function*

Cross PSD function of spatial ground motions at point k and l on ground surface can be written as:

$$S_{\ddot{u}_k \ddot{u}_l}(\omega) = \sqrt{S_{\ddot{u}_k \ddot{u}_k}(\omega) S_{\ddot{u}_l \ddot{u}_l}(\omega)} \gamma_{kl}(\omega), \tag{14}$$

where $\gamma_{kl}(\omega)$ is the coherency loss function. The adopted coherency loss function is derived from the theoretical model of Luco and Wong [1986], as:

$$\gamma_{kl}(\omega, x_{kl}) = \exp\left\{-\left(\frac{\gamma \omega d_{kl}}{v_s}\right)^2\right\} \exp\left\{-i\omega \frac{d_{kl}^L}{v_{app}}\right\}, \tag{15}$$

in which γ is an incoherence factor, d_{kl} denotes the horizontal distance between stations k and l, d_{kl}^L denotes the projected horizontal distance in the longitudinal direction of propagation of waves, v_s is the shear wave velocity of the medium, and v_{app} is the surface apparent wave velocity.

The coherency factor γ is a measure of the loss coherency rate with the distance and frequency, and its range definition is based on the empirically derived values of the ratio [Luco *et al.*, 1986],

$$\frac{\gamma}{v_s} = q \times 10^{-4}, \tag{16}$$

in which v_s is the shear wave velocity in the medium. According to the observations of some field data, Luco and Wong [1986] suggested the ratio q as $2 \leq q \leq 3$, which can be assumed as a reasonable value for a medium level of correlation between the ground motions. When $\gamma/v_s \to 0$, the first term of Eq. (15) tends to be one and the coherence effect results from wave traveling only. If $v_{\text{app}} \to \infty$, then the second term of Eq. (15) tends to be one and the incoherence is due to the geometric incoherence only.

In this study $q = 2.5$ parameter value is used for partially correlated. v_{app} is taken as $200, 400, 800$, and $1600\,\text{m/s}$ for the soft, medium soft, medium firm, and firm soil conditions, respectively.

3.3. *Determination of stochastic earthquake ground motion model parameters*

The stochastic model parameters of earthquake ground motion can be obtained based on the Code for Design of Seismic of Electrical Installations (GB 50260-96) [Ministry of China Electrical Industry, 1996]. Kaul [1978] suggested a simple formula that makes such a transformation. Its precision was recently found to be not quite satisfactory [Lin *et al.*, 2004], and so the following procedure is adopted instead, as follows:

(1) Approximately select the initial values of the input PSD $S_i^0(\omega_i), i = 0, 1 \ldots, n$.
(2) For any single-degree-of-freedom (SDOF) vibrator with the natural frequency θ_i and damping ratio ς, the expected maximum absolute acceleration response under a given PSD $S(\omega)$ of stationary random excitation is:

$$A_m(\theta_i) = p\sigma_0(\theta_i), \tag{17}$$

in which

$$\sigma_0(\theta_i) = \left[\int_0^\infty S(\omega)\frac{1 + 4\varsigma^2(\omega/\theta_i)^2}{[1 - (\omega/\theta_i)^2]^2 + 4\varsigma^2(\omega/\theta_i)^2}d\omega\right]^{\frac{1}{2}}, \tag{18}$$

$$p = \sqrt{2\ln(\nu\tau)} + 0.577/\sqrt{2\ln(\nu\tau)}, \tag{19}$$

where $\nu = \frac{1}{\pi}\sqrt{\lambda_2/\lambda_0} \approx \theta_i/\pi, \lambda_j = \int_0^\infty \omega^j S(\omega)d\omega$, τ is the duration of the earthquake.
(3) The calculation formula of the absolute acceleration under the non-stationary input is given by:

$$A_m(\theta_i) = p\sqrt{M}\sigma_0(\theta_i), \tag{20}$$

where $M = [-(32 + \sqrt{2})t_1/40 + t_2 + 3/(8c)]/T_d$, in which t_1 and t_2 are defined as the ramp duration and the decay starting time, c is the attenuation coefficient, and T_d is defined as the vibration time of more than 50% of the peak intensity.

(4) Compute the $A_m(\theta_i)$ for $i = 0, 1 \ldots, n$ and by letting $\theta_i = \omega_i$, check their errors compared to the demands $R(\theta_i)$ due to the response spectrum method to obtain

$$E(\omega_i) = \frac{|R(\omega_i) - A_m(\omega_i)|}{R(\omega_i)} \times 100\%. \tag{21}$$

Stop the iterative procedure when, for all i, $E(\omega_i) < 2.0\%$. Otherwise modify $S(\omega_i)$ by using:

$$S_i^{(k+1)}(\omega_i) = S_i^{(k)}(\omega_i) R_a^2(\omega_i)/A_m^2(\omega_i), i = 0, 1, \ldots, n \tag{22}$$

and then repeat steps (2)–(4).

(5) Using the nonlinear fitting technique, the stochastic model parameters can be obtained by Clough–Penzien model and generated power spectral density.

3.4. *Simulation of multi-component multi-support ground motions*

Standard stochastic ground motion simulation method is used to simulate response spectrum compatible multi-component multi-support ground motions [Hao *et al.*, 1989]. There is no difference between the simulation approach of multi-component multi-support ground motions and single-component multi-support ground motions [Tian *et al.*, 2008; Hao *et al.*, 1989]. The power spectrum matrix of single-component multi-support should be extended to the power spectrum matrix of multi-component multi-support one. Considering the spatial distribution and space correlation of earthquake ground motion random field, the spectral matrix of multi-component multi-support stationary ground motions can be expressed as:

$$[S(\omega)] = \begin{bmatrix} S_{11}(\omega) & \cdots & S_{1i}(\omega) & \cdots & S_{1k}(\omega) \\ \vdots & \ddots & \vdots & \ddots & \vdots \\ S_{i1}(\omega) & \cdots & S_{ii}(\omega) & \cdots & S_{ik}(\omega) \\ \vdots & \ddots & \vdots & \ddots & \vdots \\ S_{k1}(\omega) & \cdots & S_{ki}(\omega) & \cdots & S_{kk}(\omega) \end{bmatrix}, \quad (i = 1, \ldots, k) \tag{23}$$

where k is the number of support points, $S_{ii}(\omega)$ is the spectral matrix of the ith point of single-support multi-component stationary ground motions, and $S_{ij}(\omega)(i, j = 1, \ldots, k,\ i \neq j)$ is the multi-component cross-spectral density matrix of the ith point and jth point.

Figure 8 shows the displacement fields of multi-component multi-support ground motions on the medium firm soil condition with $\alpha = 0.0°$. Figure 9 shows the longitudinal, transverse, and vertical comparisons between simulated and target power spectrum. Figure 10 shows the comparison between simulated and target coherency loss function. As can be seen from these figures, the simulated ground motions are compatible with the target response spectrum and the coherency loss function.

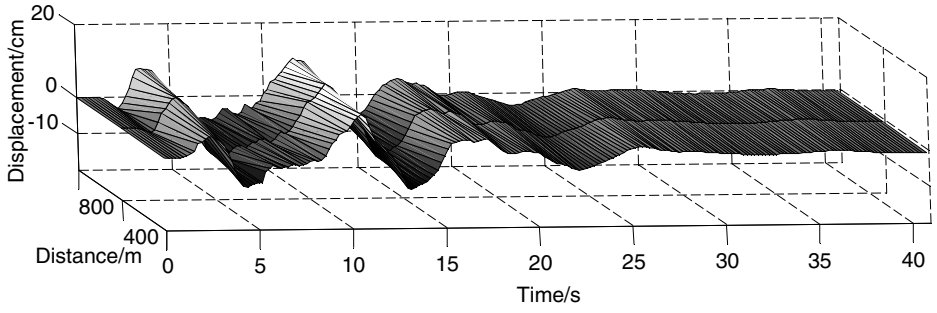

(a) Displacement fields of longitudinal multi-support ground motions.

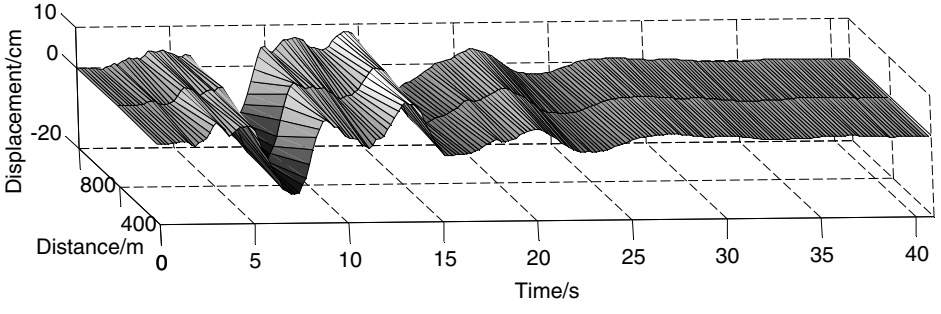

(b) Displacement fields of transverse multi-support ground motions.

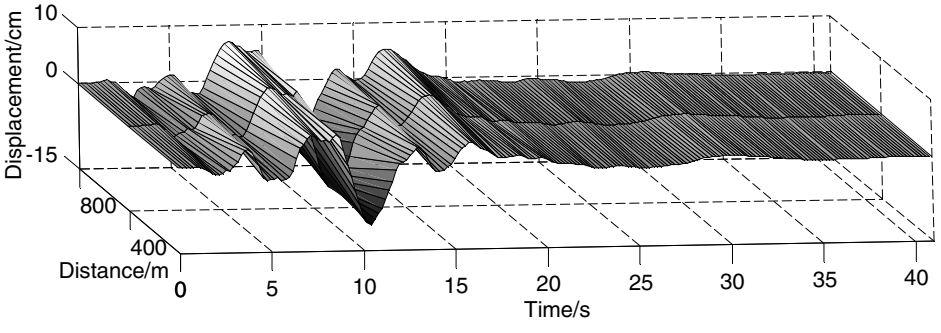

(c) Displacement fields of vertical multi-support ground motions.

Fig. 8. Displacement fields of multi-component multi-support ground motions.

4. Equations of Motion of the Transmission Tower-Line System Subjected to Multi-Component Multi-Support Excitations

Non-linear dynamic time history analysis of transmission tower-line system concludes two steps. Firstly, the geometric non-linear of transmission tower-line system under a static dead load is analyzed, and the configuration and stress of final state of static analysis are obtained. Secondly, the configuration and stress of final state

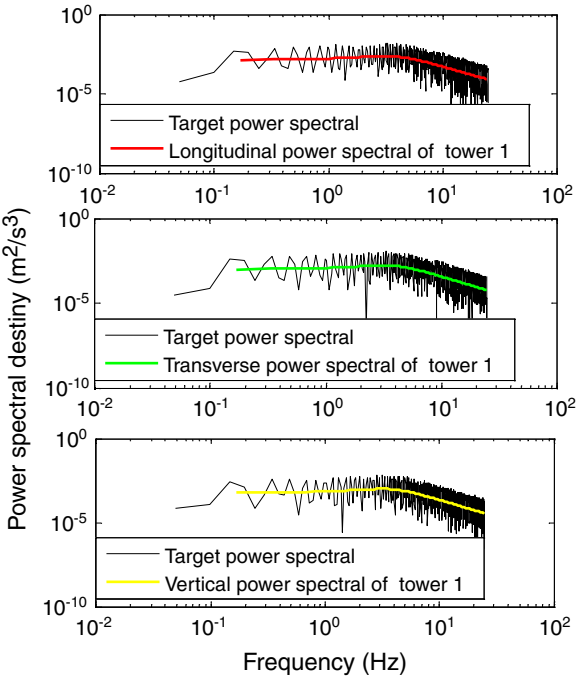

Fig. 9. Comparison between simulated and target power spectrum.

of static analysis are used as the initial state of geometric non-linear dynamic time history analysis. Then, according to equations of motion of system subjected to multi-component multi-support excitations and step by step integration method, the seismic responses of system are obtained.

n-degree-of-freedom linear system subjected to m support motions can be written in the matrix form [Wilson, 2002]

$$\begin{bmatrix} \mathbf{M}_{aa} & \mathbf{M}_{ba} \\ \mathbf{M}_{ab} & \mathbf{M}_{bb} \end{bmatrix} \begin{Bmatrix} \ddot{x}_a \\ \ddot{x}_b \end{Bmatrix} + \begin{bmatrix} \mathbf{C}_{aa} & \mathbf{C}_{ba} \\ \mathbf{C}_{ab} & \mathbf{C}_{bb} \end{bmatrix} \begin{Bmatrix} \dot{x}_a \\ \dot{x}_b \end{Bmatrix} + \begin{bmatrix} \mathbf{K}_{aa} & \mathbf{K}_{ba} \\ \mathbf{K}_{ab} & \mathbf{K}_{bb} \end{bmatrix} \begin{Bmatrix} \dot{x}_a \\ \dot{x}_b \end{Bmatrix} = \begin{Bmatrix} 0 \\ \mathbf{P}_b(t) \end{Bmatrix}, \tag{24}$$

where $x_a = [x_{a1}, \ldots, x_{an}]^{\mathrm{T}}$ is the n-vector of displacements at the unconstrained degrees of freedom. $x_b = [x_{b1}, \ldots, x_{bn}]^{\mathrm{T}}$ is the m-vector of prescribed support displacements. $\mathbf{M}_{aa}, \mathbf{C}_{aa}$, and $\mathbf{K}_{aa}$ are the $n \times n$ mass, damping and stiffness matrices associated with the unconstrained degrees of freedom, respectively. $\mathbf{M}_{bb}, \mathbf{C}_{bb}$, and $\mathbf{K}_{bb}$ are the $m \times m$ matrices associated with the supported degrees of freedom. $\mathbf{M}_{ab}, \mathbf{C}_{ab}$, and $\mathbf{K}_{ab}$ are the $n \times m$ coupling matrices associated with both the sets of degrees of freedom, and $\mathbf{P}_b(t)$ is the m-vector of the reacting forces at the support degrees of freedom.

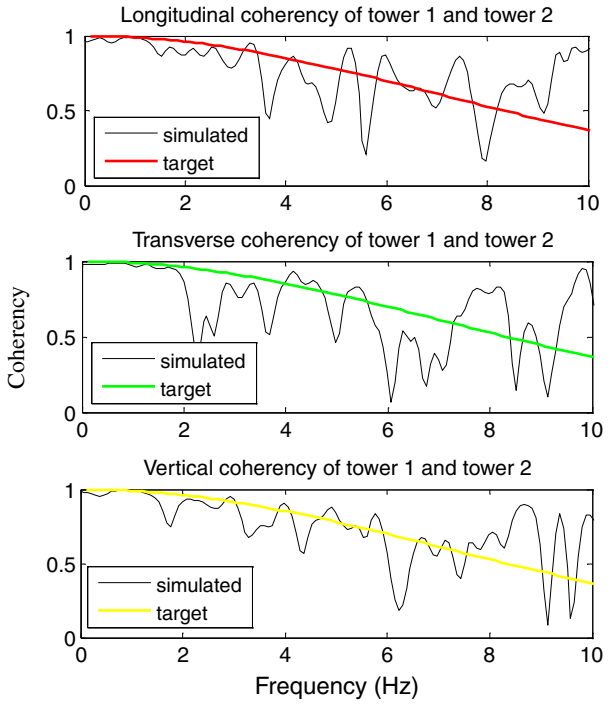

Fig. 10. Comparison between simulated and target coherency loss function.

The equation defining the response degrees of freedom "a" is given by:

$$\mathbf{M}_{aa}\ddot{x}_a + \mathbf{C}_{aa}\dot{x}_a + \mathbf{K}_{aa}x_a = -\mathbf{M}_{ab}\ddot{x}_b - \mathbf{C}_{ab}\dot{x}_b - \mathbf{K}_{ab}x_b. \tag{25}$$

The solution of Eq. (25) depends on how the earthquake motion is defined in the right-hand side of the equation.

Equation (25) is the equation of motion for the absolute displacement. Assuming that the mass matrix is diagonal and $\mathbf{C}_{ab}$ is neglected, Eq. (25) can be expressed as:

$$\mathbf{M}_{aa}\ddot{x}_a + \mathbf{C}_{aa}\dot{x}_a + \mathbf{K}_{aa}x_a = \mathbf{K}_{ab}x_b. \tag{26}$$

Equation (26) can be extended to three components

$$\mathbf{M}_{aa}\ddot{u}_a + \mathbf{C}_{aa}\dot{u}_a + \mathbf{K}_{aa}u_a = \mathbf{K}_{ab}(x_b + y_b + z_b), \tag{27}$$

where x_b, y_b, and z_b are the input ground motion displacements in two horizontal and one vertical directions, respectively. According to the research by Liu *et al.* [2009], there has been a problem in current input displacement model. Thus, the appended massless rigid element method which was put forward by Liu *et al.* [2010] is adopted in this study.

5. Parametric Study

Non-linear responses of the transmission tower-line system shown in Fig. 3 subjected to multi-component multi-support excitations are calculated. The damping ratio of tower and cable are assumed to be 2% and 1%, respectively. The step-by-step integration of the Hilber–Hughes–Taylor method is used in the dynamic analysis. The integration time step is taken to equal 0.005 s which was established to be small enough to obtain adequate accuracy and convergence. To examine the multi-component multi-support ground motions effect, the maximum axis force, shear force and moment at the bottom elements of middle tower, the maximum displacement at the top nodes of middle tower, and the maximum tension in each layer of transmission lines are studied. The ratio of the peak values of the three-component of multi-support multi-component ground motions is taken as $1:0.85:0.65$, and the maximum acceleration value of the ground motion is taken as 0.2 g. The major principal axis of ground motion coincides with the direction of wave propagation, and the direction of wave propagation along the longitudinal direction of the system, unless mentioned otherwise. The transmission tower-line system is assumed to locate on the medium firm soil unless mentioned otherwise.

5.1. *Effect of single-component multi-support ground motions and multi-component multi-support ground motions*

To investigate the effect of single-component multi-support ground motions and multi-component multi-support ground motions, four cases, i.e., longitudinal-component multi-support ground motions (Case 1), transverse component multi-support ground motions (Case 2), vertical component multi-support ground motions (Case 3), and multi-component multi-support ground motions (Case 4) are considered to calculate the transmission tower-line system responses.

The responses under single-component multi-support excitations and multi-component multi-support excitations are shown in Table 4. The brackets of Table 4 show the percentage between the response under single-component excitation and corresponding to the response under multi-component excitations. The responses under multi-component excitations (Case 4) are obviously higher than the responses under single-component excitation (Case 1, Case 2, and Case 3), especially the

Table 4. The responses of tower and lines induced by single-component multi-component ground motions and multi-component multi-support ground motions.

	Condition	Case 1	Case 2	Case 3	Case 4
Tower	Axis force (kN)	160.78(93%)	77.47(45%)	60.06(35%)	172.31
	Shear force (kN)	6.50(89%)	3.35(46%)	2.49(34%)	7.34
	Moment (kN·m)	6.85(87%)	3.71(47%)	2.60(33%)	7.86
Line	(1) Tension (kN)	16.16(96%)	13.94(83%)	14.37(86%)	16.78
	(2) Tension (kN)	102.68(98%)	88.30(84%)	90.36(86%)	104.70
	(3) Tension (kN)	104.11(97%)	88.13(82%)	90.62(85%)	107.07
	(4) Tension (kN)	107.50(97%)	87.99(79%)	91.17(82%)	111.17

responses considering vertical component excitation only (Case 3). As shown in Table 3, the longitudinal component of ground motion (Case 1) has the most significant influence on the system responses owing to the coupled effect of the tower-line system. Therefore, multi-component ground motions cannot be neglected in seismic response analysis of transmission tower-line system.

5.2. *Effect of the correlations among three-component of multi-component multi-support ground motions*

To study the effect of the correlations among three-component of multi-component multi-support ground motions, four cases, i.e., (a) $\alpha = 0.0°$, (b) $\alpha = 18.0°$, (c) $\alpha = 45.0°$, and (d) completely correlated, are considered to calculate the system responses. A special case that the three components of ground motion are completely correlated is considered in the study.

Table 5 shows the response of tower subjected to the four cases with different correlations among three-component of multi-component multi-support ground motion. As can be seen, the higher is the correlations among three-component of ground motion, the larger is the structural responses. Ignoring the correlations among the three-component of ground motions, the calculation results may be small. Assuming the correlations among three-component of ground motions are completely correlated will lead to a little large response of tower. Usually, the correlations among three-component of ground motion will not be completely correlated. The above observations indicate that the correlations among three-component of ground motions can be neglected when calculating the tower responses.

5.3. *Effect of the spatial correlation of multi-component multi-support ground motions*

To investigate the spatial correlation, three cases of multi-component multi-support ground motions, i.e., uncorrelated, partially correlated, and fully correlated, are used as input to calculate the structural responses.

Table 6 shows the response of tower subjected to the three cases with different correlation of multi-component multi-support ground motions. As shown in Table 6, increase the spatial correlation of multi-component multi-support ground motions, the responses of tower increase, indicating the uncorrelated ground motion results

Table 5. The responses of tower induced by the correlations among three-component of multi-component multi-support ground motions.

	Condition	$\alpha = 0.0°$	$\alpha = 18.0°$	$\alpha = 45.0°$	Completely correlated
Tower	Axis force (kN)	172.31	177.17	179.23	185.28
	Shear force (kN)	7.34	7.43	7.46	7.53
	Moment (kN·m)	7.86	7.95	7.98	8.03
	Displacement (cm)	7.92	8.09	8.16	8.25

Table 6. The response of tower induced by the spatial correlation of multi-component multi-support ground motions.

	Condition	Uncorrelated	Partially correlated	Fully correlated
Tower	Axis force (kN)	201.86	172.31	152.56
	Shear force (kN)	9.05	7.34	6.61
	Moment (kN·m)	9.98	7.86	7.02
	Displacement (cm)	7.95	7.92	6.08

in the highest responses of all cases. The reason for this is attributed to the contribution of the quasi-static part of the response. For partially correlated ground motion, the responses are in between the two cases. In order to obtain a representative analysis, the degree of spatial correlation of multi-component multi-support ground motions is needed to consider.

5.4. *Effect of the incident angle of multi-component multi-support seismic waves*

Assuming the angle between the direction of wave propagation and longitudinal direction of transmission tower-line system is β as shown in Fig. 11. The incident angle of multi-component multi-support seismic waves is studied by varying the direction of seismic wave propagation with respect to the longitudinal direction of the tower-line system.

Relationship curves between the maximum responses of transmission tower and the incident angle of seismic wave are shown in Fig. 12. As can be seen, the effect of the incident angle of seismic wave has a significant effect on the responses of transmission tower, especially for the tower axis force. Assuming the direction of wave propagation coincides with the longitudinal direction of the transmission tower-line system could not obtain the maximum responses of transmission tower.

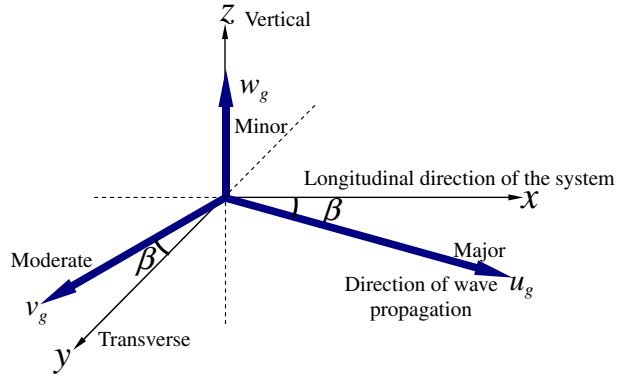

Fig. 11. Layout of the direction of wave propagation and the direction of the system.

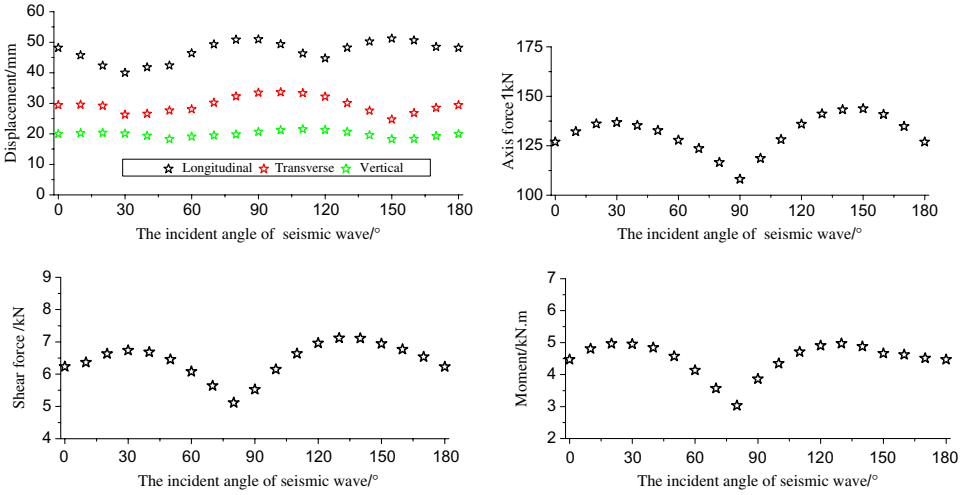

Fig. 12. Relationship curves between the maximum responses of transmission tower and the incident angle of seismic wave.

5.5. *Effect of the ratio of the peak values of the three-component of multi-component multi-support ground motions*

Five different ratios of the peak values of the three-component of ground motion ($R_u : R_v : R_w$), i.e., (a) 1 : 1 : 1, (b) 1 : 1 : 0.5, (c) 1 : 0.85 : 0.65, (d) 0.85 : 1 : 0.65, and (e) 0.65 : 1 : 0.65 are considered in this study. All ratios are calculated with respect to a reference acceleration of 0.2 g. The maximum acceleration value of the ground motion is taken as 0.2 g, and the acceleration values of the other two components are obtained according to the above ratios. The direction of wave propagation (u) is assumed to coincide with the longitudinal direction of the transmission tower-line system.

The responses under different ratios of the peak values of the three-component of ground motion excitation are shown in Table 7. As can be seen, the ratios of the peak values of the three-component of ground motion have a significant effect

Table 7. The responses of tower and lines induced by the ratio of the peak values of three-component of multi-component multi-support ground motions.

	Condition	1:1:1	1:1:0.5	1:0.85:0.65	0.85:1:0.65	0.65:1:0.65
Tower	Axis force (kN)	179.20	173.21	172.31	154.65	136.83
	Shear force (kN)	7.85	7.38	7.34	6.70	5.91
	Moment (kN·m)	8.51	7.96	7.86	7.31	6.46
	Displacement (cm)	8.47	7.66	7.92	6.91	5.59
Line	(1) Tension (kN)	16.64	16.45	16.78	16.22	15.60
	(2) Tension (kN)	105.95	104.34	104.70	102.70	99.92
	(3) Tension (kN)	108.56	106.59	107.07	104.71	101.43
	(4) Tension (kN)	113.05	110.50	172.31	108.20	104.15

on the response of tower and lines. It is observed that a relative reduction in the vertical component and an increase in the longitudinal component may increase the responses of tower and lines. It is also obvious from the table that a relative increase in the transverse component and a reduction in the longitudinal component may reduce the responses of system. Thus, the relative magnitude of the longitudinal component of ground motion determines the magnitude of the dynamic responses in the tower and lines.

5.6. *Effect of site condition and apparent wave velocity of multi-component multi-support ground motion*

Four different sets of site conditions and wave velocities of ground motion, i.e., the firm soil with $v_{\text{app}} = 1200\,\text{m/s}$ (Case 1), the medium firm soil with $v_{\text{app}} = 800\,\text{m/s}$ (Case 2), the medium soft soil with $v_{\text{app}} = 400\,\text{m/s}$ (Case 3), and the soft soil with $v_{\text{app}} = 200\,\text{m/s}$ (Case 4) are considered in this study.

Table 8 shows the responses of tower and lines under different site condition and apparent wave velocity of ground motion excitation. It is seen from the table that the responses of case 4 are obviously larger than those of other cases. The reason of this is attributed to the higher energy contents of the spectrum at frequencies corresponding to the first few modes of the tower that coupled with lines, which contributes maximum to the response. The energy contents of the spectrum at case 3 frequencies are less compared to those of case 4, which lead to a significant decrease in response. For case 2, which corresponds to the medium firm soil with $v_{\text{app}} = 800\,\text{m/s}$, the responses are drastically decreased since the energy contents of the spectrum at these frequencies are significantly less. Especially for case 1, the responses are the smallest of all cases.

These observations indicate that the site condition and apparent wave velocity of multi-component multi-support ground motions significantly influence the responses of the tower and lines. Therefore, it is important to consider the local site condition and apparent wave velocity on ground motion in transmission tower-line system analysis and design.

Table 8. The responses of tower and lines induced by site condition and apparent wave velocity of multi-component multi-support ground motions.

	Condition	Case 1	Case 2	Case 3	Case 4
Tower	Axis force (kN)	106.72	172.31	359.68	508.10
	Shear force (kN)	4.84	7.34	15.23	21.62
	Moment (kN·m)	5.16	7.86	16.04	23.13
	Displacement (cm)	4.19	7.92	20.00	31.40
Line	(1) Tension (kN)	15.60	16.78	22.73	22.28
	(2) Tension (kN)	99.62	104.70	117.50	115.81
	(3) Tension (kN)	99.27	107.07	113.55	131.28
	(4) Tension (kN)	100.89	111.17	124.15	133.20

6. Conclusions

This paper study the seismic response of transmission tower-line system subjected to multi-component multi-support excitations. The effects of single-component multi-support ground motions, multi-component multi-support ground motions, correlations among the three-component of multi-component multi-support ground motions, the spatial correlation of multi-component multi-support ground motions, the incident angle of multi-component multi-support seismic waves, the ratio of the peak values of the three-component of ground motion, and site condition and apparent wave velocity of multi-component multi-support ground motions on the responses of the transmission tower-line system are investigated. The results of the parametric study lead to the following conclusions:

(1) The responses of the transmission tower-line system under multi-component multi-support excitations are obviously higher than those of system under single-component multi-support excitations. The responses of system are governed by the longitudinal component of ground motion.
(2) The higher is the correlations among three-component of ground motion, the larger is the system responses. The degree of the correlations among three-component of ground motion is carried out by changing the angle between the direction of major principal axis and the direction of wave propagation. The influence of the degree of the correlations among three-component of ground motion on the system responses is not obvious.
(3) The lower is the spatial correlation of ground motion, the larger is the structural responses. In order to obtain a representative analysis, the degree of the spatial coherency of multi-component multi-support ground motions is needed to consider.
(4) The incident angle of multi-component multi-support seismic waves has a significant effect on the responses of system. The direction of wave propagation is assumed to coincide with the longitudinal direction of the transmission tower-line system could not obtain the maximum responses of transmission tower.
(5) The ratio of the peak values of the three-component of multi-component multi-support ground motions have considerable effects on the response of the system. The relative magnitude of the component which coincides with the longitudinal direction of the transmission tower-line system determines the magnitude of the dynamic responses in the tower and lines.
(6) Different site condition and apparent wave velocity of ground motion also have a significant influence on transmission tower-line system responses.

Owing to the complexity of the large span structure, it is very difficult to give general conclusions from the researches on a single transmission tower-line system model. However, results from this study demonstrate the importance of considering the above parameters on seismic responses of transmission tower-line system. More

studies are deemed to further investigate the multi-component multi-support effect on responses of the transmission tower-line system.

Acknowledgments

This project is supported by the National Natural Science Foundation of China under grant No. 50638010 and the Foundation of Ministry of Education for Innovation Group under Grant No. IRT0518. This support is greatly appreciated.

References

American Society of Civil Engineers Committee on Electrical Transmission Structures. [1982] "Loadings for electrical transmission structures," *ASCE J. Struct. Div.* **108**(5), 1088–1105.

American Society of Civil Engineers. [1991] "Guideline for electrical transmission line structural loading," *ASCE Manuals and Reports on Engineering Practice,* New York, USA.

Clough, R. W. and Penzien, J. [1975] *Dynamics of Structures* (McGraw-Hill, New York, USA).

Ghobarah, A., Aziz, T. S. and El-Attar, M. [1996] "Response of transmission lines to multiple support excitation," *Eng. Struct.* **18**(12), 936–946.

Huadong Electrical Power Design Institute. [1999] *State Electrical Power Company, Design Regulation on* $110 \sim 500\,kV$ *Overhead Transmission Line (DL/T* 5092–1999) (China Electrical Power Press, Beijing, China).

Hall, J. F., Holmes, W. T. and Somers, P. [1995] "Northridge earthquake of January 17, 1994," *Earthquake Engineering Research Institute*, California, USA.

Hao, H., Oliveira, C. S. and Penzien, J. [1989] "Multiple-station ground motion processing and simulation based on SMART-1 array data," *Nucl. Eng. Des.* **111**, 1325–1345.

Kaul, M. K. [1978] "Stochastic characterization of earthquakes through their response spectrum," *Earthquake Eng. Struct. Dyn.* **6**(5), 497–510.

Li, H. N., Shi, W. L. and Jia, L. G. [2003] "Simplified aseicmic calculation method considering effects of line on transmission tower," *J. Vibr. Eng.* **16**(2), 233–237.

Li, H. N. [2006] *Theoretical Analysis of Structures to Multiple Earthquake Excitations* (Scientific Press, Beijing, China).

Li, H. N., Shi, W. L. and Jia, L. G. [2004] "Limitations of effects of lines on in-plane vibration of transmission towers and simplified seismic calculation method," *Vibr. Impact* **23**(2), 1–7.

Li, H. N., Shi, W. L., Wang, G. X. *et al.* [2005] "Simplified models and experimental verification for coupled transmission tower-line system to seismic excitations," *J. Sound Vibr.* **286**(3), 565–585.

Lin, J. H., Zhang, Y. H., Li, Q. Sh. *et al.* [2004] "Seismic spatial effects for long-span bridges using the pseudo excitation method," *Eng. Struct.* **26**, 1207–1216.

Liu, G. H., Li, H. N. and Lin, H. [2009] "Comparison and evaluation of models for structural seismic responses analysis," *Eng. Mech.* **26**(2), 10–15.

Liu, G. H., Li, H. N., Guo, W. *et al.* [2010] "A new method for solving problem of current displacement input model for calculating structural seismic responses," *Eng. Mech.* **27**(9), 55–62.

Luco, J. E. and Wong, H. L. [1986] "Response of rigid foundation to a spatially random ground motion," *Earthquake Eng. Struct. Dyn.* **14**, 891–908.

Ministry of China Electrical Industry. [1996] *Code for Seismic Design of Electrical Facilities* (GB 50260-96) (China Plan Press, Beijing, China).

Mozer, J. D. *et al.* [1977] "Longitudinal load analysis of transmission line system," *IEEE Trans. Power Apparatus Syst.* **96**(5), 1657–1665.

Penzien, J. and Watable, M. [1975] "Characteristics of 3-dimensional earthquake ground motions," *Earthquake Eng. Struct. Dyn.* **4**, 365–373.

Shen, S. Z., Xu, C. B. and Zhao, C. [1997] *Design of Suspension Structure* (China Architecture and Building Press, Beijing, China).

Shinozuka, M. [1995] "The Hanshin-Awaji earthquake of January 17, 1995 performance of life lines," *Report NCEER-95-0015*, NCEER.

Tian, L., Li, H. N. and Huang, L. Zh. [2008] "Lateral response of transmission tower-line system under multiple support excitations," *Proc. Chin. Soc. Electr. Eng.* **28**(6), 108–114.

Tian, L., Li, H. N. and Liu, G. H. [2010] "Seismic response of power transmission tower-line system subjected to spatially varying ground motions," *Mathematical Problems in Engineering*, 2010, Article ID 587317.

Wilson, E. L. [2002] "Three Dimensional Statics and Dynamic Analysis of Structures: A Physical Approach with Emphasis on Earthquake Engineering," *Computer and Structures*, Berkley, California, USA.

Yasui, H., Marukawa, H. and Momomura, Y. *et al.* [1999] "Analytical study on wind-induced vibration of power transmission towers," *J. Wind Eng. Ind. Aerodyn.* **83**(2), 431–441.

Yin, R. H., Li, D. L., Liu, G. L. *et al.* [2005] "Seismic damage and analysis of power transmission towers," *World Earthquake Eng.* **21**(1), 51–54.